EFFECT OF CROSS WIND ON AERODYNAMIC COEFFICIENTS OF GROUND VEHICLES

Vihar Malviya, Naresh Gundala, Rakesh Mishra
University of Huddersfield, Queensgate, Huddersfield HD1 3DH, UK

ABSTRACT

The present work investigates the variation of aerodynamic coefficients with the change in the angle of flow. A mathematical equation has been developed for predicting the aerodynamic coefficients, when a vehicle is subjected to crosswind. A tractor-trailer model has been utilised to demonstrate the effectiveness of the proposed equations. Flow analysis was carried out using Computational Fluid Dynamics (CFD) software. CFD simulations have been carried out on the tractor-trailer model at a wind speed of 25 m/s, for wind angles ranging from 0° to 180° . The computational results obtained have been used for comparing the predicted aerodynamic coefficients. This mathematical model developed can be used for various aerodynamic investigations that involve large angles of attack.

Keywords: Aerodynamics, analytical model, coefficient, flow angle, CFD

INTRODUCTION

The modern developments in automotive engineering have shown a trend to develop faster, more efficient and light-weight vehicles. These design considerations unfortunately are in contrast to a stable behaviour in strong crosswinds. There have been incidents reported, that some heavy vehicles and also trains were turned over while operating in strong crosswinds. There has been a lack of research on vehicles in the actual transient wind environments experienced on the road. The external flow field determines the aerodynamic forces and moments, which determine the vehicle stability behaviour in side winds. Baker (1987) had set out a general analysis on the wind-induced vehicle accidents which also provided the information about the vehicle aerodynamic coefficients over a wide range of yaw angles. Baker (1986) has developed a four-wheeled single-mass vehicle model, applied it to a bus-accident, where he noticed that, the aerodynamic coefficients were the least well defined parameters. The side coefficients appear very large as the coefficients for the high-sided road vehicles were referred to the frontal area rather than the side area. He also stated that 'the force and moment coefficients show quite a large degree of sensitivity to changes in the modelling technique'. He also noticed that there were similarities in wind flow patterns over high-sided vehicles to wind patterns observed on building roofs. Suzuki et al. (2003) have discussed how some of the aerodynamic coefficients vary with the cross winds. It was also noticed that while the aerodynamic characteristics were visualised at low speed under a range of yaw angles, the airflow was extremely turbulent and vortical in the leeward side. The aerodynamic coefficients for a tractor-trailer on a bridge, based upon the computational fluid mechanics were presented by Bettle (2003). It can be seen from the above discussion that most attempts at predicting both aerodynamic and non-aerodynamic stability have been based on a large number of assumptions, including those for calculating aerodynamic coefficients. It is hence required to quantify the aerodynamic coefficients based on generic parameters such as vehicle dimensions. This paper presents a methodology to accurately quantify the influence of angle of attack of flow on the aerodynamic coefficients of a vehicle by mathematical equation; this investigation also involves numerically simulating flow over a vehicle model by using Computational Fluid Dynamic (CFD) code *Fluent* (Fluent Inc. 2006). The investigation proposes to achieve a generic relation between aerodynamic coefficients and flow angle with a focus on its application in a vehicle stability model for a wide range of vehicles.

METHODOLOGY

As mentioned earlier, this paper aims to develop a set of equations to predict the aerodynamic coefficients for vehicles travelling in cross wind conditions at large angles of attack. The predicted coefficients have then been compared with those obtained by Computational Fluid Dynamics (CFD) simulations. To study how the change in flow angle affects the aerodynamic coefficients flow angle was changed from 0° to 180°. A study on how the aerodynamic coefficients change with respect to the frontal and projected areas was performed. The experimental results obtained during an earlier research (Malviya et al. 2009) were used to validate the CFD results obtained in the present work.

Aerodynamic Forces

Equations for predicting aerodynamic forces are well known. They are influenced by the frontal area of the vehicle as the characteristic area because the frontal area represents the region on which the oncoming flow impacts. Thus drag force (F_D), lift force (F_L) and side force (F_S) can be represented by the following equations:

$$F_D = \frac{\rho C_D A_{FRONT} v^2}{2} \quad (1)$$

$$F_L = \frac{\rho C_L A_{FRONT} v^2}{2} \quad (2)$$

$$F_S = \frac{\rho C_S A_{FRONT} v^2}{2} \quad (3)$$

Here C_D, C_L and C_S represent the Drag, Lift and Side-force coefficients respectively and A_{FRONT} is the characteristic frontal area, ρ is the air density and v is the air speed. For large flow angles the frontal area is no longer the area on which the flow impacts and does not fully characterise the aerodynamic forces.

Characteristic Area

The area influenced by the impact of oncoming flow characterises the aerodynamic forces and moments created by the external flow field for large angles of flow. This has been taken to be the area of the front and side faces projected normal to the flow itself. The projected areas can also be found using the relative yaw angle (φ) of the flow, length (l), width (w) and height (h) of the tractor-trailer model.

The projected area of the indicating surface of the side = $(l \cdot \sin\varphi) \cdot h$ (4)

The projected area of the indicating surface of the front = $(w \cdot \cos\varphi) \cdot h$ (5)

The total projected area of the indicating surface can be written as an equation, which can be formed using the projected areas of both the front and side of the vehicle.

$$A = projected\ area\ of\ the\ side + projected\ area\ of\ the\ front$$

$$A = (l \cdot \sin\varphi + w \cdot \cos\varphi) \cdot h \quad (6)$$

Aerodynamic Coefficients

The aerodynamic forces, combined with the characteristic area used, were used to calculate the aerodynamic coefficients. So,

$$C_D = \frac{2F_D}{\rho \times [(l.\sin\varphi + |w.\cos\varphi|) \times h] \times v^2} \quad (7)$$

$$C_L = \frac{2F_L}{\rho \times [(l.\sin\varphi + |w.\cos\varphi|) \times h] \times v^2} \quad (8)$$

$$C_S = \frac{2F_S}{\rho \times [(l.\sin\varphi + |w.\cos\varphi|) \times h] \times v^2} \quad (9)$$

Also, the rolling moment (M_R), pitching moment (M_P) and the yawing moment (M_Y) can be found using the following equations

$$C_R = \frac{2M_R}{\rho \times [(l.\sin\varphi + |w.\cos\varphi|) \times h_{CG}] \times v^2} \quad (10)$$

$$C_P = \frac{2M_P}{\rho \times [(l.\sin\varphi + |w.\cos\varphi|) \times h_{CG}] \times v^2} \quad (11)$$

$$C_Y = \frac{2M_Y}{\rho \times [(l.\sin\varphi + |w.\cos\varphi|) \times h_{CG}] \times v^2} \quad (12)$$

Here (h_{CG}) is height of the centre of gravity of the vehicle which is the characteristic length.

CFD SIMULATIONS

The aerodynamic coefficients predicted by the proposed equations were required to be compared against a validated benchmark to ensure accuracy of these predictions. CFD simulations were carried out on a full scale tractor-trailer model and the results were used for comparison. The results obtained by CFD were validated against a set of results obtained from earlier research (Malviya et al. 2009). The simulation of flow

around the tractor-trailer was performed for different angles (φ) ranging from 0° to 180° with a relative wind velocity (v_{REL}) of 25 m/s. The tractor-trailer considered was 16.28 m long, 2.6 m wide and 4.3 m high; it was based on earlier research to establish a basis for comparison of the predicted aerodynamic coefficients. The aerodynamic coefficients were computed for each case of flow angle considered. The wheels of the model with a rolling radius of 0.19485 m rotate at an angular velocity corresponding to the longitudinal (x) component of the flow velocity about the respective axles/axes. The x- and z-components of the relative velocity vector are computed using the following equations:

$$u_x = -v_{REL} \cdot \cos\varphi \quad (13)$$

$$u_z = v_{REL} \cdot \sin\varphi \quad (14)$$

Computational Domain

Fluid domains were created around the tractor-trailer model. The larger domain (179 × 50 × 22 m) was used to capture the essential flow features. A smaller domain consists of a rectangular cuboids' volume 179 m × 18.2 m × 22 m (Malviya et al. 2009) which contains the tractor-trailer model as shown in the figure. The length of the domain was 179m, such that the inlet of the flow domain was flow domain was $3 \cdot l$ upstream of the developed tractor-trailer. The outlet of the domain was $7 \cdot l$ downstream of the model which is spatially sufficient to prevent the downstream-imposed constant pressure of 101325 Pa (ambient atmospheric pressure) from having an upstream effect on the pressure field. The width of the flow domain was 18.2 m, such that the longitudinal side walls of this domain were at a distance of $3 \cdot w$ from the model, which was found sufficient to prevent the domain wall boundary layer with the flow-field of the model. Also, the height of the flow domain was 22 m such that the distance between the top surface of the semi-trailer and the horizontal top wall of the domain was at least $4 \cdot h$.

Mesh

Tet/Hybrid meshing scheme was used to discretise the computational fluid domain into about 2.6 million finite volumes. The maximum skewness of the meshed geometry was 0.79 and for most of the elements it was about 0.6.

Boundary Conditions and Continuum

Suitable boundary conditions and Continuum were assigned to the meshed geometry. These are listed below:

- Wall: For stationary edges and faces
- Velocity Inlet: Velocity of air flow is 25 m/s; turbulent viscosity ratio was set to 10 and Turbulent Intensity to 5%
- Pressure outlet: The outlet was set to atmospheric (101325 Pa)
- Interior: used for the inner faces of smaller domain
- Road is a moving wall and wheels are set as rotating wall
- Continuum around the tractor-trailer was fluid

CFD Parameters

For numerical simulation of the flow two popular two-equation turbulence models were considered, the *realizable k-ε* and the *SST k-ω* models. Both these models are claimed to predict with reasonable accuracy the characteristics of separated flow. An earlier comparison of these two turbulence models was carried out by the authors to investigate the external flow around a tractor-trailer combination (Malviya et al. 2009); it was found that the *SST k-ω* model predicted the flow characteristics with a better accuracy. Hence *SST k-ω* was chosen for the analysis.

Validation of CFD Results

The obtained CFD results were compared with a previous research (Malviya et al. 2009) on a similar model. A vertical rake was created at $0.2 \times l$ upstream of the front face of the cab of the model to obtain the pressure distribution. The model investigated during the previous research was a 1:40 scale model of the tractor-trailer combination. The point of measurement was located 0.08 m upstream of the front face of the cab of the model, which corresponds to a full scale distance of 3.24 m. The vertical height y above the

ground has been converted to non-dimensional form relative to the height of the semitrailer ($h_{trailer}$), and measured from the bottom of the vehicle. On the Y-axis is the Co-efficient of Pressure (C_p) and on the X-axis is the vertical height from the bottom of the semi-trailer. As the height increases the pressure co-efficient decreases and we can observe that the maximum value is at the bottom of the semi-trailer. Experimental values obtained in the earlier research are seen to be about 0.05 higher near the bottom of the tractor-trailer; this could be attributed to experimental errors and inaccuracies. The results from the CFD and experiment match well, which provide sufficient accuracy for the purpose of this present work.

RESULTS AND DISCUSSIONS

The analysis of flow around the tractor-trailer model was performed. From the obtained results pressure distribution on the different faces of the tractor-trailer model and also the comparison of the variation of non-dimensional coefficients with the wind angle were discussed.

Distribution of Pressure

Over 90% of the drag force is due to the pressure drag, which is caused due to the non-uniformity of the pressures acting on the vehicle, so in order to analyse the pressure differences on the vehicle, the pressure distribution contours of different faces were taken and discussed below. The pressure values measured across the flow domain were represented in non-dimensional form by using the expression for coefficient of pressure (C_p) as

$$C_p = \frac{p - p_\infty}{q_\infty} \tag{15}$$

Where

p ≡ local static pressure
p_∞ ≡ free-stream static pressure
q_∞ ≡ free-stream dynamic pressure

If U_∞ is the free-stream velocity, then

$$q_\infty = \frac{1}{2}\rho U_\infty^2 \tag{16}$$

Fig 4 shows distribution of pressure on the front face of the tractor cab, the rear face of the semitrailer and the side face of the entire tractor-trailer with the flow at 45°. Fig 4(a) shows the pressure distribution on the rear face of the trailer. It can be observed that there is a smaller region with a high pressure value of -0.162 at the bottom of the right end of the trailer (left end of the figure) and as we move away from the right end towards the left end there is a decrease in the pressure where a low pressure value of -0.48 can be observed at the top of the trailer. Also a non-dimensional line can be observed in the trailer which represents the partitioning line that was generated due to the grid partition in the Fluent.

It is observed from Fig 4 (b), that there is a high pressure value of 0.965 both at the left side end of the cab and trailer (right side end of the cab and trailer in the figure) and as we from the left end to the right end we can observe that the pressure value gradually decreased to -0.881 at the right end of the trailer (left side end of the trailer in the figure). Also large region of constant pressure can be observed in the middle of the trailer and also it is nearly symmetrical about the horizontal centre line. Also a non-dimensional line can be observed in the trailer which represents the partitioning line that was generated due to the grid partition in the Fluent. From the Fig.4(b), it can be predicted that the pressure distribution is nearly symmetrical about the horizontal centre line. It can be observed that there is a large region of high pressure value $(C_p\ more\ than\ 0.136)$ at the right side of the cab (left side of the figure) and there is a low pressure value of -1.5 at the left side end (right side of the figure). As we move from the right side end to left side end we can observe the decrease in the pressure values.

Variation of Non-Dimensional Coefficients with the Wind Angle

The faces of the vehicle model exposed to the oncoming flow were projected onto imaginary planes normal to the flow and the areas were computed. These computed projected areas at different flow angles were then used to compute aerodynamic coefficients in the CFD simulations.

COEFFICIENT OF DRAG FORCE

Figure 5 shows the variation of drag coefficient with the flow angle using the obtained CFD results both with respect to frontal area and the projected area. Drag coefficient predicted by using the proposed equations has also been shown. It is observed that the coefficients predicted using the proposed equation match well with the CFD results. At a relative flow angle of 0° , C_D with respect to the CFD projected area was found to be 0.89 and at an angle of 75° the value of C_D went down to 0.0216 and it was further decreased to a value of -0.9399 at an angle of 180°. With respect to the proposed equation, C_D at a flow angle of 0° was found to be 0.84 and it went down to a value of 0.0183 at an angle of 75° and then further decreased to a value of -0.89 for the flow at 180°. Also with respect to the CFD frontal area, there is a gradual decrease in the C_D values as the flow changes from 0° to 180°.

COEFFICIENT OF LIFT FORCE

Fig 6 shows the variation of lift coefficient with the flow angle using the obtained CFD results both with respect to frontal area and the projected area. Also, lift coefficients predicted by using the proposed equations were used to compare to that of the obtained CFD results. At a relative flow angle of 0°, C_L with respect to the CFD projected area was found to be 0.0335 and at an angle of 30° the value of C_L was increased to 0.4813 and it was decreased to a value of 0.0103 at an angle of 75° and then increased to a value of 0.4621 at an angle of 150° and finally decreased to a value of 0.0298 for the flow at 180°. With respect to the proposed equation, C_L at a flow angle of 0° was found to be 0.0318 and it was increased to a value of 0.428 at an angle of 30° and then it was decreased to a value of 0.0087 at an angle of 75° and then increased to a value of 1.18 at an angle of 165° and finally decreased to a value of 0.0283 for the flow at 180°. Also with respect to the CFD frontal area, there are gradual fluctuations observed in the C_L values as the flow changes from 0° to 180° as show in the Fig. 6.

COEFFICIENT OF SIDE FORCE

Fig 7 shows the variation of side-force coefficient with the flow angle. C_S is found to be zero at a flow angle of 0° and the value of C_S increased to a value of 1.3386 and it is seen from the figure that it remains almost constant and then found to be zero at an angle of 180°. These values are with respected to the CFD projected area and with respect to the proposed equation, the value of C_S gradually increased almost from 0 to 1.174 and it remained constant up to a flow angle of almost 165° and then found to be zero at an angle of 180°. With respect to the frontal area, C_S is zero at a flow angle of 0° and it gradually increased to a value of 6.51 at an angle of 75° and then was found to be zero at the flow angle of 180° .

CONCLUSIONS

The present work provides the variation of non-dimensional aerodynamic coefficients with the flow angles ranging from 0° to 180° . A mathematical equation has been developed to determine the aerodynamic coefficients under different flow conditions. The results computed from the CFD with respect to projected area match well with the results obtained by using the mathematical equation developed. By this, we can conclude that the developed mathematical equation is able to predict the non-dimensional aerodynamic coefficients for a range of relative flow angles. Thus, this equation can be applied to various aerodynamic investigations that involve large angles of attack.

REFERENCES

Baker, C., (1986). 'A simplified analysis of various types of wind-induced road vehicle accidents'. *Journal of Wind Engineering and Industrial Aerodynamics*, 22(1), pp.69-85.

Baker, C., (1987). 'Measures to control vehicle movement at exposed sites during windy periods'. *Journal of Wind Engineering and Industrial Aerodynamics*, 25(2), pp.151-161.

Bettle, J. et al., (2003). 'A computational study of the aerodynamic forces acting on a tractor-trailer vehicle on a bridge in cross-wind'. *Journal of Wind Engineering and Industrial Aerodynamics*, 91(5), pp.573-592.

Fluent Inc., (2006). 'FLUENT 6.3 User's Guide'.

Malviya, V. et al., (2009). 'CFD Investigation of a Novel Fuel-Saving Device for Articulated Tractor-Trailer Combinations'. *Engineering Applications of Computational Fluid Mechanics*, 3(4), pp.587-607.

Suzuki, M. et al., (2003). 'Aerodynamic characteristics of train/vehicles under cross winds'. *Journal of Wind Engineering and Industrial Aerodynamics*, 91(1-2), pp.209-218.

Figures

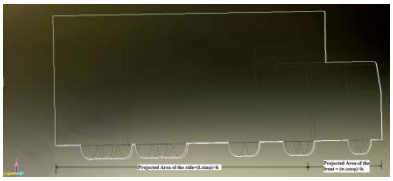

Figure 1: Projected area of the indicating surface at a particular flow angle

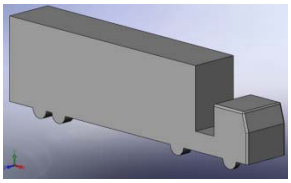

Figure 2: Tractor-trailer combination (Malviya et al. 2009)

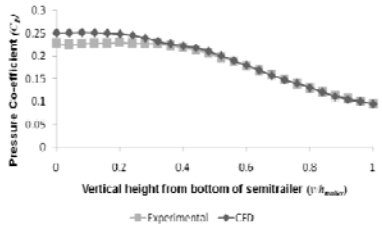

Figure 3: Comparison of pressure profiles along a vertical rake upstream of tractor-trailer

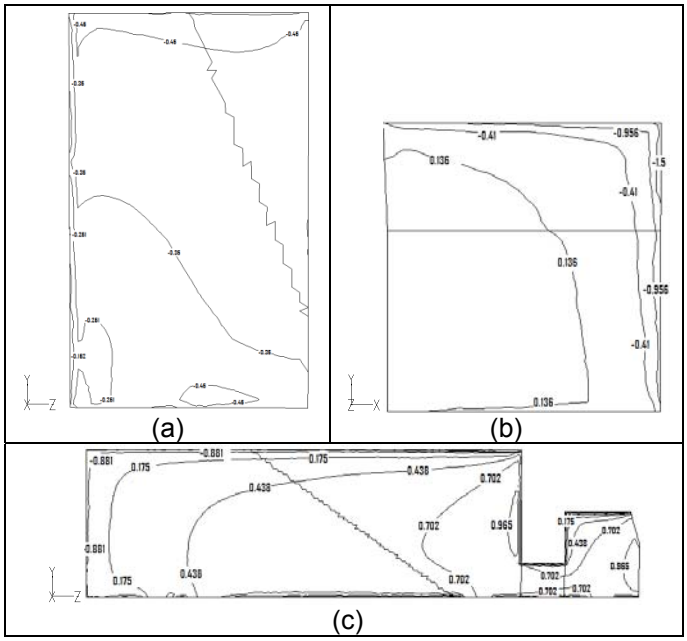

Figure 4: Pressure distribution for 45° flow on the (a) rear (b) front and (c) side faces of the tractor-trailer

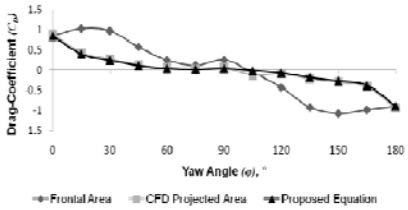

Figure 5: Variation of drag coefficient with flow angle

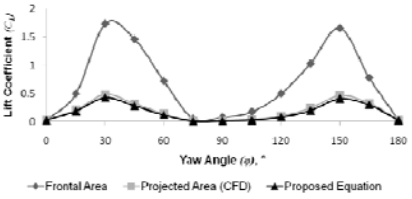

Figure 6: Variation of lift coefficient with flow angle

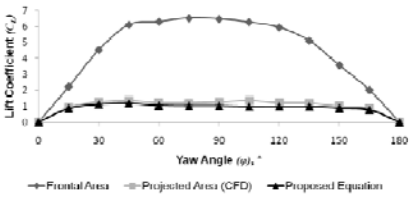

Figure 7: Variation of side-force coefficient with flow angle